Advanced Steel Construction – Vol. 18 No. 2 (2022) 544–551
DOI:10.18057/IJASC.2022.18.2.3

PROPAGATION MODE AND CHARACTERISTICS OF FATIGUE CRACKS IN STEEL BRIDGE DECK AFTER DRILLING AHEAD OF THE CRACK TIP

Liang Fang [1], Zhong-Qiu Fu [1,*], Bo-Hai Ji [1] and Shigenobu Kainuma [2]

[1] *College of Civil and Transportation Engineering, Hohai University, Nanjing, China*
[2] *Department of Civil Engineering, Kyushu University, Fukuoka, Japan*
** (Corresponding author: E-mail: fuzhongqiu@hhu.edu.cn)*

ABSTRACT

Drilling the stop-hole ahead of the crack is a common maintenance method when the crack tip cannot be accurately identified or the crack length is short with a narrow operating space. The fatigue test and finite element simulation were conducted to study the crack-propagation mode and stress characteristics of the stop-hole after drilling. By monitoring the hole-edge strain, combined with simulation results and experimental phenomena, the reason for the change of crack-growth direction and path after drilling ahead of the tip was explained. Local stress characteristics of the fatigue crack before and after drilling ahead were compared to explore the influence on crack propagation. The result shows that the stop-hole will crack in advance while the original crack has not reached hole edge and two cracks will propagate in opposite direction at a rapid rate until they meet. The stop hole can guide the crack to propagate towards the stress concentration zone in front of hole edge, which is the reason for crack turning at the hole. Drilling ahead of the crack increases the stress intensity factor at the crack tip by 15% to speed up crack propagation and weaken the arresting effect. However, crack retardation can still be observed after the original crack converges with the crack initiating from hole.

ARTICLE HISTORY

Received: 6 June 2021
Revised: 11 August 2021
Accepted: 11 August 2021

KEYWORDS

Steel bridge deck;
Fatigue crack;
Drilling ahead;
Propagation mode;
Hole edge strain

1. Introduction

Steel box girder is often used as the main beam of bridge, especially in long-span bridges, due to its advantages of light weight, high torsional strength, good wind resistance, convenient fabrication and construction [1,2]. However, out-of-plane deformation in different directions can occur in the steel bridge deck under the cyclic loadings, leading to fatigue crack initiation [3-5]. With the advantages of high efficiency, economy and convenience, the stop-hole is widely used in the maintenance of fatigue cracks [6-8] and the hole location is an important technical parameter that affects the effect while drilling.

In the process of drilling the stop-hole, the crack tip is unevenly distributed along the thickness of the component for the irregular shape of the crack, and the crack tips sometimes failed to be completely removed as shown in Fig. 1(a). Meanwhile, it is difficult to accurately determine the specific location of crack tip by the existing detection equipments due to the cracking of surface coating and internal defects in the component. Even if the crack tip on upper surface is located, the hole is still prone to be drilled behind the tip, as shown in Fig. 1(a). The crack appears as a short crack growing from the hole, which has an abnormal high growth rate [9]. In addition, a number of cracks in the real bridge initiate from the weld, and don't extend to the roof or U-rib. The stop-hole drilled at the roof or U-rib can weaken the local bearing capacity , as shown in Fig. 1(b). Besides, the crack length is usually short and distributes in the narrow space between components in the real bridge. Considering the narrow operation space for personnel and equipment as well as the implementation of post-processing such as hole edge grinding, it is proposed to drill the stop-hole ahead of the crack tip based on the predication of the crack-growth path. This method has been applied to the maintenance of fatigue cracks in several long-span cable supported bridges. Therefore, although the hole position $d = 0.5D$ (D to the hole diameter) recommended by scholars [10,11] and the manual [12] can theoretically achieve a better effect while drilling, in practice, considering the difficulty in determining the crack tip, it is often inevitable to drill ahead of the crack.

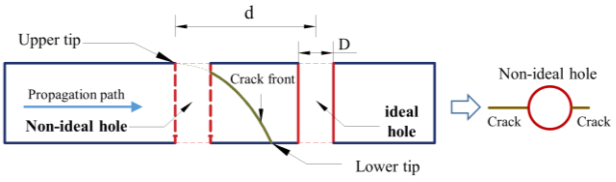

(a) Non-ideal hole 1

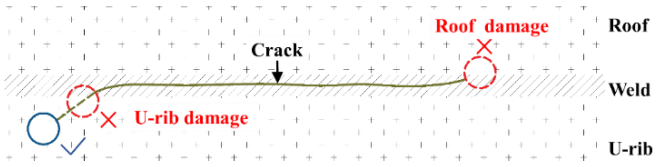

(b) Non-ideal hole 2

Fig. 1 Non-ideal hole morphology

Shin et al. [9] found that when a hole is drilled at a certain distance before the crack tip, the crack can also extend into the hole, which reduces the difficulty in identifying the crack tip and has a certain effect of delaying the crack growth. The feasibility of drilling ahead of the crack was confirmed. Wang et al. [13] drilled holes within the distance of d=1.0t (t to the thickness of specimens) from the crack tip and find that the stress peak at the hole edge decreased with increasing of hole position. It is indicated that hole-edge stress is greatly affected by the drilling position. Hu et al. [14] studied the relationship between the hole position and the crack-growth direction by establishing a numerical model. The result shows that drilling holes within a reasonable distance in vertical and horizontal directions near the crack tip can obtain the maximum crack-propagation angle and change the crack-growth direction. Makabe et al. [15] also found that drilling ahead of the crack tip can guide cack propagation, preventing multiple cracks from converging to cause greater section damage. The above studies all show that drilling ahead has the engineering feasibility and can play a role in changing the crack-growth direction.

In addition, during the inspection of steel box girder in suspension bridges, engineers find that the fatigue crack growth morphology of some holes ahead of cracks is quite different from that of drilling at $d = 0.5D$, as shown in Fig. 2. Before the crack reaches the stop-hole, two cracks with different paths appear on the front side of the hole. The farther the crack on the front side of the hole is from the hole edge, the narrower the width. Since the width of the crack tip is usually narrow, it is speculated that the crack on the front side of the hole is not caused by the bifurcation of the original crack, but a new crack initiating from the hole. Therefore, based on the existing research and real bridge inspection, the impact of drilling ahead of the crack tip on crack-propagation mode and tip characteristics needs to be further clarified. In terms of research objects, existing literatures focus on the impact of drilling on fatigue cracks, but the effect of crack propagation on stop holes cannot be ignored. The interaction between drilling and original crack propagation also needs to be further clarified.

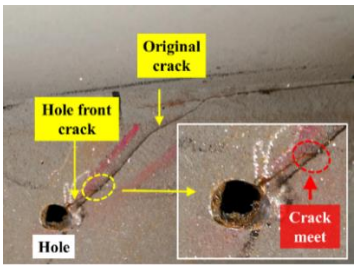

Fig. 2 Crack growth morphology after drilling ahead of the crack tip

Based on the observation of real bridge cracks, the fatigue test and numerical simulation are carried out to analyze the effects of stop-hole with hole position $d > 0.5D$ and the influence on the propagation mode of the fatigue crack. The crack-growth direction, path, stress intensity factor and the stress characteristics at the hole edge after drilling ahead of the crack tip are revealed. The conclusions obtained provide a reference for the optimization and application of the fatigue-crack arresting technology in real bridges.

2. Fatigue test

2.1. Specimen design

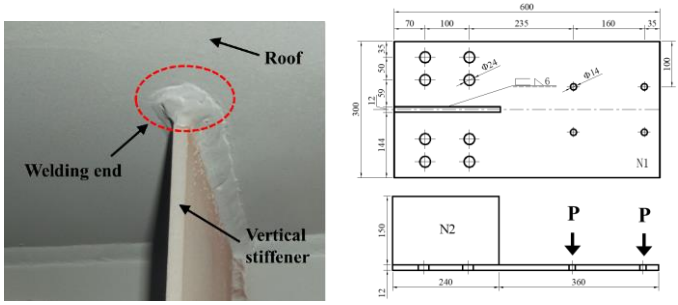

(a) Real bridge roof-vertical stiffener (b) Local full-scale specimen

Fig. 3 Local full-scale specimen of roof-vertical stiffener

In order to verify the conjecture in Fig. 1 that stop-hole drilled ahead of the crack tip results in the crack initiation at the hole edge before the original crack propagates to the hole, the constant-amplitude fatigue test of local full-scale models was designed and carried out with the roof-vertical stiffener (RVS) [16] and diaphragm U-rib (DU) [10] in steel bridge deck as the research object. The specimen was made by steel Q345qD which is the same as that of real bridges. The roof and vertical stiffening ribs are perpendicularly intersected with the T-joint wrap angle welded. The diaphragm and U-rib are girth welded at the arc notch. Due to geometric discontinuity and welding residual stress [17], high stress concentration may occur at the weld toe and root [18]. According to the observation and statistics of the real bridge, fatigue cracks are prone to initiating at the wrap angle of the girth weld in both two structures, which significantly affects the durability and safety of steel bridges [5].

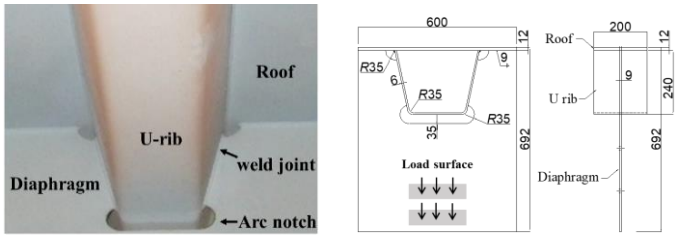

(a) Real bridge diaphragm U-rib (b) Local full-scale specimen

Fig. 4 Local full-scale specimen of diaphragm U-rib

2.2. Test conditions

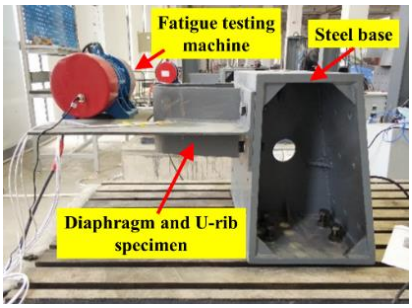

Fig. 5 Test device

Drilling tests with different hole locations were designed for DU and RVS specimens. As the crack propagated to 35mm in the 4 specimens of diaphragm U-ribs (DU), SJ4-8 and SJ4-9 were drilled at $d = 2D$ and $d = 2.5D$ ahead of the crack tip respectively, while SJ4-7 and SJ4-10 were drilled at $d = 3D$. The hole diameter D is 10mm and the loading stress amplitude is 120MPa with the stress ratio of -1. As the crack propagated to 45mm, three RVS specimens were drilled at $d = 3D$, numbered SJ3-5, SJ3-6 and SJ3-7. The other specimen SJ3-8 was drilled at $d = 2.5D$ with the loading stress amplitude of 160MP and diameter of 10mm. Fatigue tests were carried out by the fatigue testing machine (see Fig. 5) which can generate the bending load as that in real bridges. Test conditions are shown in Table 1.

Table 1
Test conditions

	Specimens	Crack length /mm	Hole location /mm	Diameter/mm	Stress amplitude /MPa
DU	SJ4-8	35	2*D*	*D*=10	120
	SJ4-9	35	2.5*D*	*D*=10	120
	SJ4-7	35	3*D*	*D*=10	120
	SJ4-10	35	3*D*	*D*=10	120
RVS	SJ3-5	45	3*D*	*D*=10	160
	SJ3-6	45	3*D*	*D*=10	160
	SJ3-7	45	3*D*	*D*=10	160
	SJ3-8	45	2.5*D*	*D*=10	160

3. Testing results and analysis

3.1. Validation of hole location effectiveness

The farthest hole position d in the test is $3D$. The result shows that fatigue cracks can effectively propagate to the hole edge under all testing conditions. Whether the crack can reach the hole is mainly affected by the angle between the crack tip and hole. Therefore, in CAD, two tangent lines were drawn from the crack tip to hole edge and the angle θ between the tangent line was calculated under different hole positions. As shown in Fig. 6, the angle θ decreases with the increase of hole position d. The first derivative curve can reflect the change of angle. When the hole position d exceeds $3D$, the derivative curve tends to be flat, indicating the small and stable decrease of angle at this stage. Therefore, it is theoretically and experimentally effective to drill holes within $d \leq 3D$, which can ensure the cracks propagating to the hole edge.

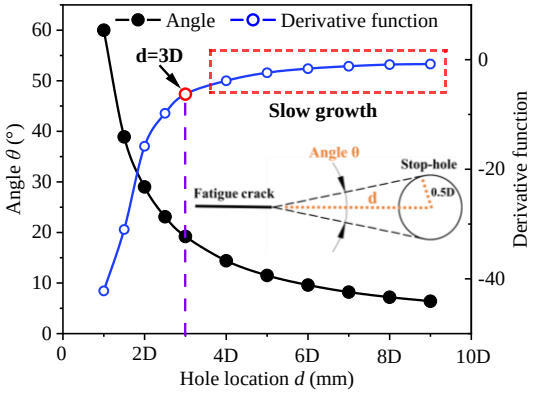

Fig. 6 Relationship between angle and hole position

3.2. Crack-propagation law

In the fatigue test of two typical details, it was observed that the crack growth-rate was barely changed at the initial stage after drilling ahead of the crack tip. However, the growth rate and morphology changed obviously as the crack propagated to the front side of the hole. Taking SJ3-6 as an example, the crack experienced 102.38 thousand loading cycles from drilling to reach the stop-hole with the propagation distance of 25 mm. During this period, the crack length increased sharply when it extended to 6.5mm away from the hole edge and then reached the hole after only 1.64 thousand loading cycles. The increased crack length in this steep-rise stage accounts for 26% of 25mm, but its duration only accounts for 1.7% of the cycles. Similarly, for SJ4-10, the crack growth in the steep-rise stage is 13 mm, accounting for 52% of 25 mm, but its duration is only 15%.

Left-crack propagation was measured in SJ4-9 after the right crack extended to the hole edge. It can be seen in Fig. 7(c) that after drilling at d = 2.5D, the crack-growth rate of the left did not have obvious change. However, when the right crack reached hole edge (Fig. 7(c) line 1), the growth rate of the left crack increased sharply and the specimen accelerated to failure.

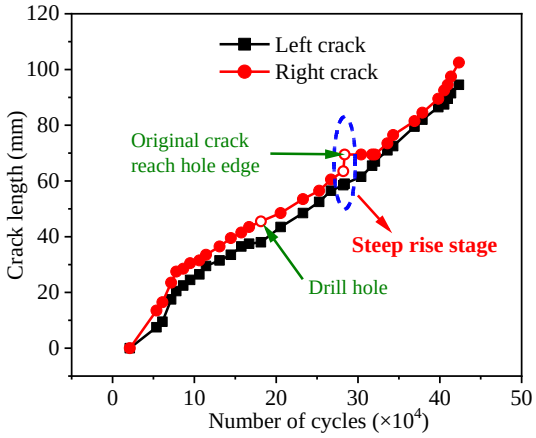

(a) RVS SJ3-6

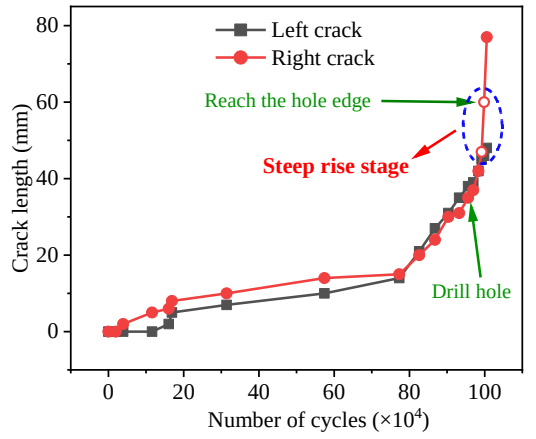

(b) DU SJ4-10

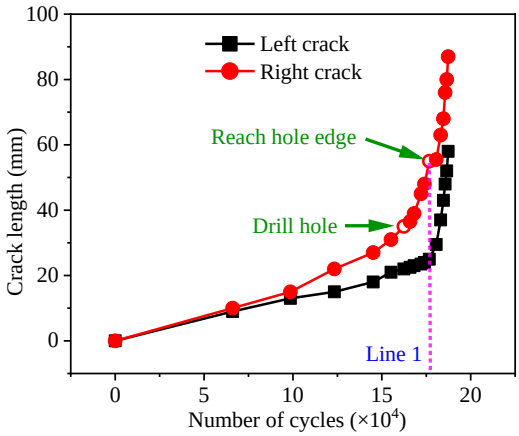

(c) DU SJ4-9

Fig. 7 Crack growth in the test

It is found that the fatigue crack "turns" before reaching the hole edge with change of crack-growth direction. As shown in Fig. 8(a), the original fatigue crack deflects nearly 75 ° before reaching the hole. Fig. 8(b) shows that the crack-growth direction changes nearly 80 ° to reach the hole. Fig. 8(c) has two narrow and connected crack tips in front of the hole. The crack morphology in Fig. 8(d) is similar to that in real bridges in Fig. 2 as the crack initiating from the hole converging with the original crack. It can be seen from the above phenomena that the original crack appears to directly propagate to the hole edge. In fact, before the original crack arrives, the front side of hole cracks ahead of time. Then the crack at stop-hole propagates opposite to the original crack until they meet.

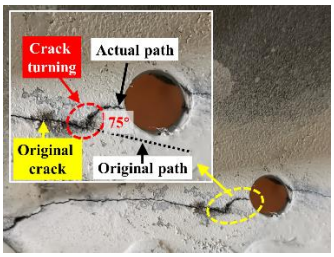

(a) SJ3-5

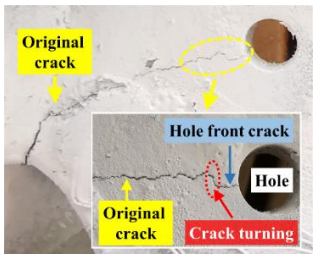

(b) SJ4-8

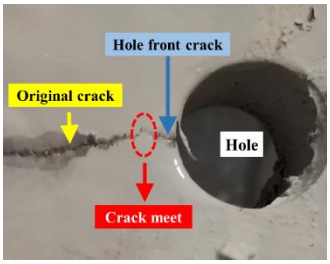

(c) SJ3-8

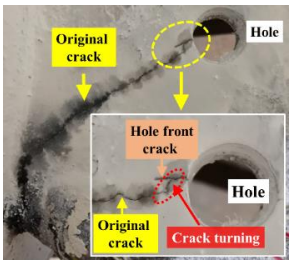

(d) SJ4-10

Fig. 8 Fatigue crack propagation mode of specimen

3.3. Strain at hole edge

In order to further explore the mechanism of crack turning and rapid propagation rate in front of the hole, strain gauges were pasted on the hole edge for stress monitoring. For RVS and DU specimens, when the right fatigue crack extended to 45mm and 35mm respectively, strain gauges were pasted on the front and back sides of the hole in SJ3-7 and SJ4-9, as shown in Fig. 9(a) and (c). Strain gauges were also pasted at the front, back, 10mm and 20mm outside the hole in SJ3-8 and SJ4-10 to record the strain change during whole process of crack propagation, as shown in Fig. 10(a) and (b).

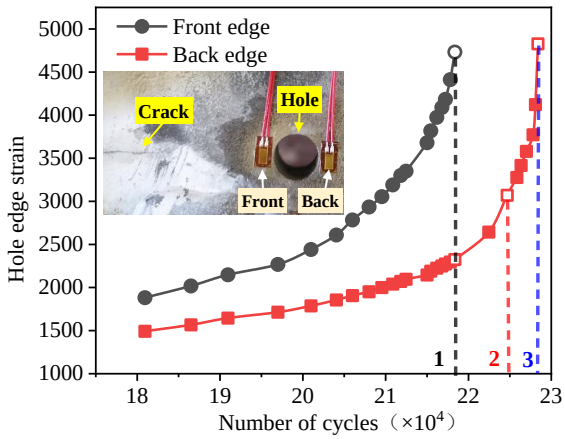

(a) Strain at front and back edge of the hole (SJ3-7)

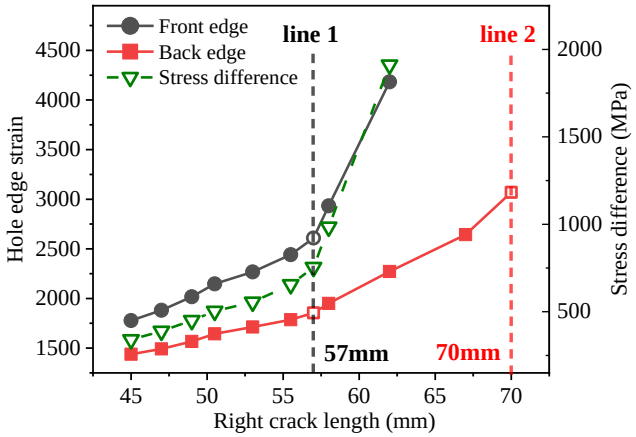

(b) Right side crack length and strain (SJ3-7)

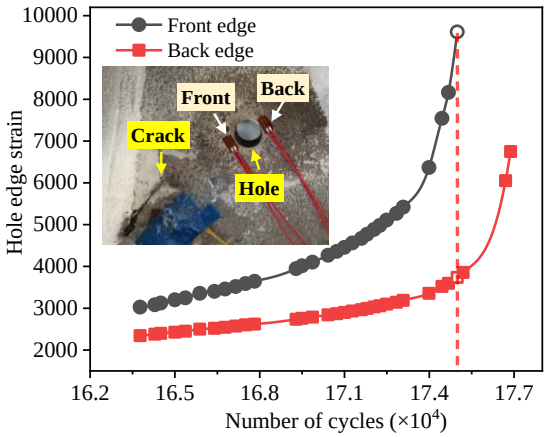

(c) Strain at the front and back of the hole (SJ4-9)

Fig. 9 Change of strain at front and back sides of the hole

Both RVS SJ3-7 and DU SJ4-9 have strain gauges pasted on both sides of the hole. Curves of strain and load cycles for the two specimens are similar, which means that strain changes on the front and back side of the hole are basically the same with the continuous growth of original fatigue cracks. Taking SJ3-7 in Fig. 9(a) as an example, dotted line 1 represents that the crack initiates on the front side of the hole and then the strain gauge fails. After that, strain-growth rate at the back of the hole continues to increase. The interval between dotted line 1 and 2 represents the opposite propagation of the original fatigue crack and the crack initiating from hole. The two cracks meet at the dotted line 2, while the original crack appears to reach the hole in the test. Dotted line 3 represents crack re-initiation at the back of the hole. Therefore, it can be seen that after drilling ahead of the crack tip, the front side of the hole will crack in advance before the fatigue crack propagates to the hole edge.

The relationship between the length of original fatigue crack and the strain at both sides of the hole was analyzed, as shown in Fig. 9(b). At the initial stage after drilling, the strain increases slowly and linearly with the growth of original fatigue cracks. When the crack extends to 57mm (13mm away from the hole edge, Fig. 9(b) Line1), the strain starts to increases rapidly. In the test, the stress amplitude measured at the crack tip near 60mm is 267MPa, which can be approximately taken as the nominal stress amplitude at the crack tip of 57mm. Fisher et al. [19] and Awad et al. [20] give the calculation formula (1) of plastic zone size when studying the fatigue performance of full-scale bridge weldments, where K_I refers to formula (2).

$$\frac{1}{2\pi}\left(\frac{K_I}{\sigma_y}\right)^2 \tag{1}$$

$$K_I = \sigma\sqrt{\pi a} \tag{2}$$

According to the formula, the radius of plastic zone near the crack tip is approximately 14.5mm. It can be seen that the plastic zone has covered the hole edge, which can explain the increase of strain-growth rate in front of the hole as the original crack propagates to 13mm away from the hole in Fig. 9(b).

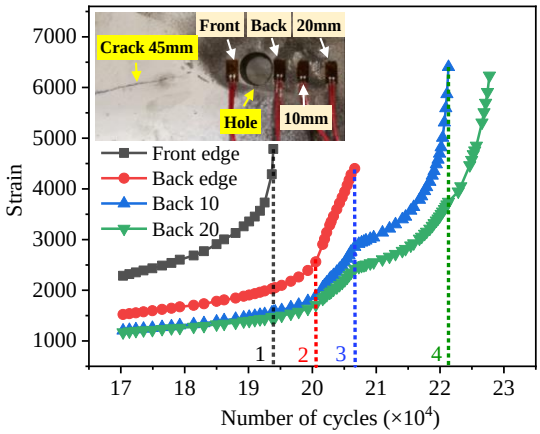

(a) RVS SJ3-8 with d = 2.5D (D=10mm)

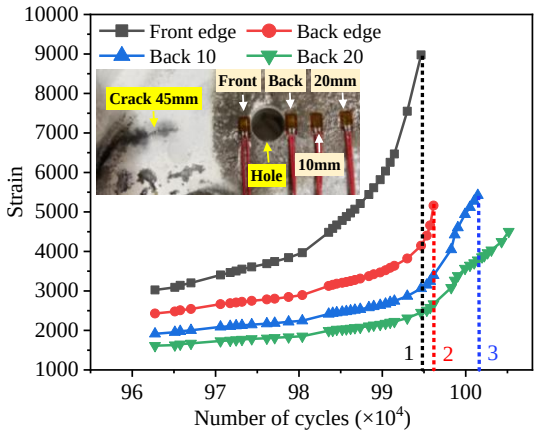

(b) DU SJ4-10 with d = 3D (D=10mm)

Fig. 10 Strain changes at the front, back, 10 mm and 20 mm of the hole

Since the strain gauge pasted in SJ3-8 and SJ4-10 are the same, SJ3-8 with more comprehensive data is selected for analysis. The physical meaning of the dotted lines 1, 2 and 3 is consistent with that in Fig. 9(a). The dotted line 4 indicates that the crack has extended to 10 mm behind the hole and the strain gauge is damaged. It can be seen from the curve that once the original fatigue crack meets the crack initiating from hole at dotted line 2, crack growth is arrested by the hole. However, the strain-growth rate at the back side, 10mm and 20mm outside the hole increases significantly (between the dotted line 2-3).

Comparing Fig. 9(a) with Fig. 10(a), it is found that when the original crack meets the crack initiating from hole, strain at the back of the hole with d = 2.5D and d = 3D is 2562 and 3070. After SJ3-8 and SJ3-7 experience 6,100 and 3720 cycles respectively, cracks are initiated from back sides of two holes. Therefore, enlarge hole position d will increase the strain at the back of hole, which weakens the crack-arresting effect as the original crack reaches hole edge.

In addition, the reason for crack turning is that there is a plastic zone at the tip of crack initiating from the hole and the original crack will propagate towards

the weak area on base metal, resulting in the change of propagation path. If the hole is drilled on the actual path of the original crack, the crack turning is not obvious, as shown in Fig. 8(c). However, if the crack-growth path is not accurately judged and the drilling is deviated, the crack turning will appear in front of the hole, as shown in Fig. 8(a), (b), (d). The hole position is upward deviated in Fig. 8(a) and (d) and is downward deviated in Fig. 8(b). Although the hole position deviates from the crack-growth path, the original crack can still effectively propagate to the hole edge. After a new crack initiating from the back side of the hole, the crack-propagation path is changed and is not on the extension line of the original crack, as shown in Fig. 8(a). This verifies that hole position has the influence on crack-growth direction.

3.4. Stress intensity factor at crack tip

The stress intensity factor (SIF) directly reflects the stress characteristics at the crack tip. The "Handbook of Stress Intensity Factors" gives a formula for calculating SIF at the crack tip near the hole edge in an infinite plate [21]:

$$K_I = F\,\sigma\sqrt{\pi a} \tag{3}$$

F is a coefficient. The crack length is $2a$. The radius of the stop hole is r. The distance from crack center to the front edge of hole and hole center is b and c respectively. It can be seen from Fig. 11 that F is positively correlated with a/b and r/c. Therefore, if the crack length and load remain unchanged, the closer the hole is to the crack tip, the larger the value of F and SIF at the crack tip are. The formula shows that SIF K_I is affected by the hole diameter D, hole position d and crack length.

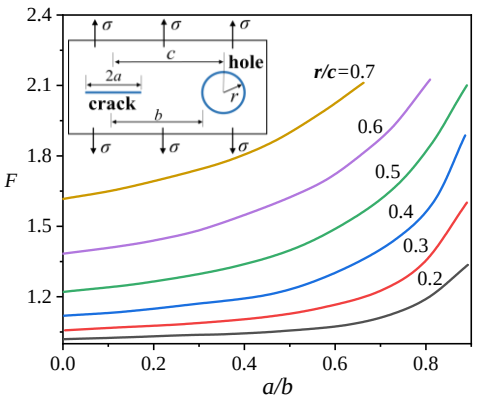

Fig. 11 The value method of coefficient F

In order to explore the influence of drilling ahead on the SIF at crack tip, the K-gage [22] method was used to measure the change of SIFs at crack tips of DU specimens SJ4-7, SJ4-8, SJ4-9 and RVS specimen SJ3-5 before and after drilling. The K-gage method is a kind of resistance strain gauge specially used to measure the SIF at the crack tip [23]. It can measure four groups of strains (ε_1 to ε_4) at the crack tip and then the mode I (K_I) and mode II (K_{II}) stress intensity factors can be calculated by formula (4), where C_1 and C_2 are constant coefficients that can be obtained by literature [24], as shown in Fig. 12.

$$K_I = C_1(\varepsilon_1+\varepsilon_2);\ K_{II} = -C_2(\varepsilon_3-\varepsilon_4) \tag{4}$$

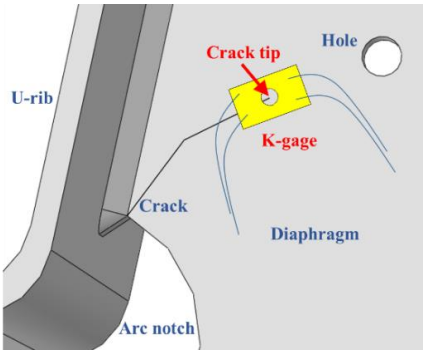

(a) Schematic diagram of K-gage pasting

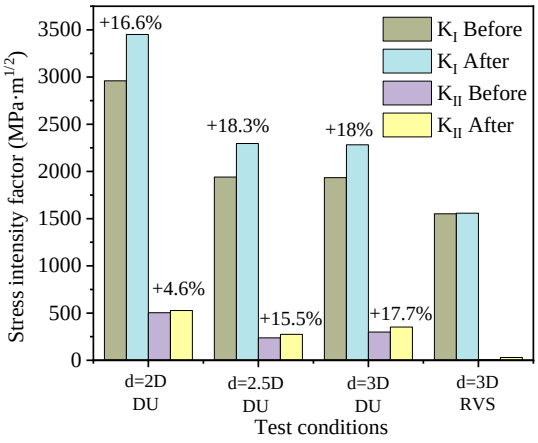

(b) SIFs before and after drilling

Fig. 12 SIF at crack tip before and after drilling

It can be seen from Fig. 12(b) that SIFs of fatigue cracks in RVS and DU specimens are dominated by K_I. The K_I and K_{II} increase after drilling ahead of the crack tip. Due to the small number of test samples, there is no obvious relationship between SIFs and the location of stop holes. The K_{II} in RVS specimen SJ3-5 after drilling ahead of the crack is 6 times of that before drilling, which is obviously beyond the common sense. It is considered that the measurement error is caused by factors such as pasting process, glue thickness and uneven surface. The average increase of K_I and K_{II} in DU specimens is 17.6% and 12.6% respectively. Therefore, for cracks propagating along the base metal in real bridges, it is suggested to drill double holes at the crack tip and d=3D, so as to remove the tip as much as possible and avoid the poor arresting effect caused by misjudgment of the crack tip.

3.5. Crack growth morphology

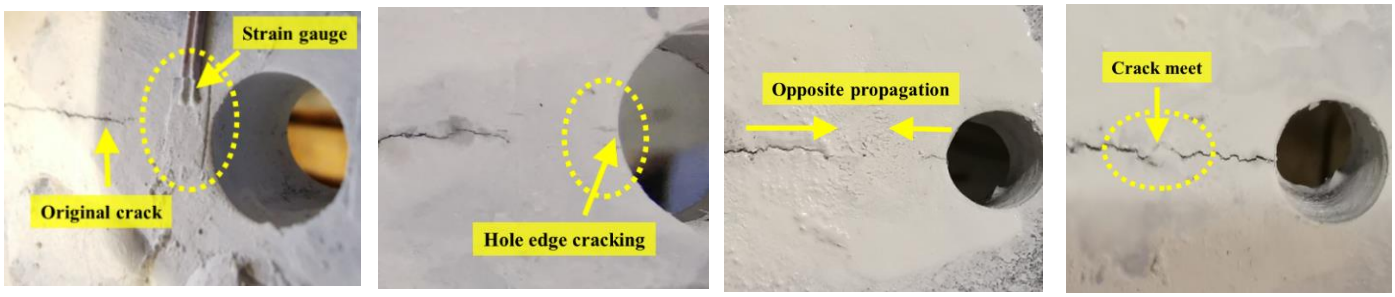

(a) Original crack (b) Hole edge cracking (c) Opposite propagation (d) Crack meet

Fig. 13 Crack-growth morphology after drilling ahead of the crack tip

During the test, the crack-growth morphology after drilling ahead of the crack was photographed and captured, as shown in Fig. 13. The crack-propagation process can be divided into four stages. Firstly, the original fatigue crack propagates continuously, and the stress in front of the hole increases slowly. When the plastic zone of the original crack covers the front edge of the hole, the growth rate of strain at the hole increases gradually, as shown in Fig. 13(a). Secondly, the crack is initiated from the base metal in front of the hole with the strain gauge damaged, while the original crack has not reached the hole edge, as shown in Fig. 13(b). Thirdly, the growth rate of the original crack is accelerated. The crack initiating from hole propagates towards the original crack

with the width increasing gradually, as shown in Fig. 13(c). Fourthly, the original crack meets the crack initiating from the hole, which is visually manifested as the original crack reaches the hole edge. After that, the growth rate of strain at the back of the hole begins to accelerate significantly.

Table 2
Comparison of crack growth rates at different stages

Specimen	S_W (mm)	$S_{3,4}$ (mm)	N_W	$N_{3,4}$	$(N_W\text{-}N_{3,4})/(S_W\text{-}S_{3,4})$	$N_{3,4}/S_{3,4}$	Magnification
SJ4-9	20	6	12930	1800	795	300	**2.65**
SJ3-7	25	5	51380	6320	2253	1264	**1.78**
SJ3-8	20	7	30870	6660	1862	951	**1.96**

The process of the crack initiating from hole to the confluence with the original crack (stage 3 to stage 4) lasts for a very short time in the test. The crack-growth rate from stage 3 to stage 4 of each specimen is shown in Table 2. The total cycle from stage 1 to stage 2 is N_W-$N_{3,4}$ with an extended distance of S_W-$S_{3,4}$, which is $N_{3,4}$ and $S_{3,4}$ for the stage 3 to stage 4. It can be seen from Table 2 that the crack-growth rate in the third and fourth stages of SJ4-9, SJ3-7 and SJ3-8 are 2.65, 1.78 and 1.96 times of that in the first and second stages with an average of more than two times. Therefore, drilling ahead of the crack indirectly accelerates the original crack to reach hole edge.

4. Finite element simulation

4.1. Modeling

The DU and RVS are similar in many aspects. Firstly, the crack-propagation mode is similar. The cracks all originate from the girth weld with symmetrical crack growth on two sides of the specimen. Secondly, the form of stress and the cause of cracking are similar. Under vehicle load, out-of-plane deformation will occur at diaphragm [25] and Roof [16], which is the most important reason for fatigue cracking. In addition, loading methods are the same in the test. Out-of-plane bending loads are both applied to two structures to create out-of-plane deformation as that in the real bridge. Therefore, the finite element simulation of DU is enough for analyzing the influence after drilling ahead of the crack tip.

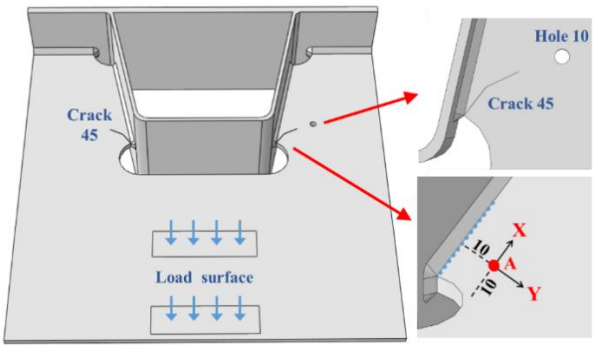

Fig. 14 Finite element model

The finite element analysis software ABAQUS was used to establish a DU model consistent with the test to drill holes ahead of the crack tip. The component size is the same as that of the fatigue test in Fig. 4. Based on the statistics of the crack-growth direction of DU specimens in the test, the "create cut" module was used to cut a seam that penetrates the base metal with the width of 0.05mm to simulate the crack in ABAQUS. According to the size of specimens, the thickness of the roof, diaphragm and U-rib of the model are 12 mm, 9 mm and 6 mm respectively. The elastic modulus of steel is 2.06 × 10^5MPa and Poisson's ratio is 0.3. Fixed constraints were imposed to the roof of the model which is the same as the boundary condition in fatigue tests. The load application surface refers to the actual contact surface between the fatigue testing machine and the specimen with a total area of 2×7380mm^2, as shown in Fig.14. By trial loading and calculation of the model without crack, the value of uniform load was set as 0.25MPa/mm^2 to ensure that the stress along Y-axis of the point A is half of the nominal stress amplitude (120MPa) in the test.

Eight-node linear hexahedral elements C3D8R and ten-node quadratic tetrahedral elements C3D10 were used for hybrid mesh division. The global grid size is 20mm. In order to analyze the stress distribution at the crack tip and hole edge, 1mm grid was used to densify the area where the crack and stop hole were located. Transition element C3D10 was adopted between the grid encrypted and unencrypted area to ensure that the grids of two areas do not affect each other, as shown in Fig.15(a).

When the crack reached 45mm, a stop-hole was drilled with the diameter D = 10mm at a distance of d = 3D from the crack tip. Taking 5mm as the interval, when the cracks were 50mm, 55mm, 60mm, 65mm, the principal stress around stop hole were extracted. Besides, a model without cracks but with a stop hole was set for comparison. The finite element model is shown in Fig. 14.

4.2. Validation of model

In order to verify the accuracy of the model, the strain gauge rosette was pasted at the same position as the model in Fig. 14 to measure the maximum principal stress amplitude of the weld toe in a crack-free state in the test, as shown in Fig. 15. Due to the symmetry of the specimen, strain gauges were pasted on both sides of the diaphragm. The maximum principal stress amplitude at the strain gauge can be calculated according to formula (5) [26].

$$\sigma_{max}=\frac{E}{2(1-\nu^2)}\left\{(1+\nu)(\varepsilon_x+\varepsilon_y)+(1-\nu)\sqrt{2\left[(\varepsilon_x-\varepsilon_u)^2+(\varepsilon_u-\varepsilon_y)^2\right]}\right\} \quad (5)$$

In formula (5), σ_{max} is the maximum principal stress. E is the elastic modulus of Q345qD steel, taken as 206 GPa. ν is the Poisson's ratio, taken as 0.3.

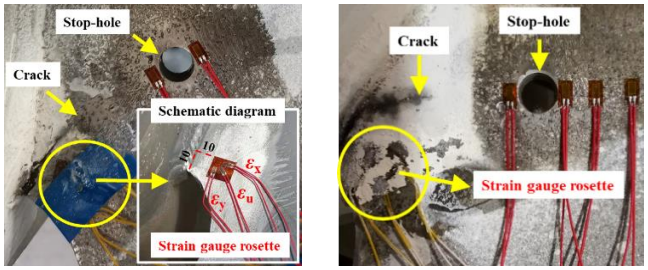

(a) SJ4-9 (b) SJ4-10

Fig. 15 Paste the strain gauge rosette at nominal stress point

The principal stress amplitude at the weld toe of specimens SJ4-7, SJ4-8, SJ4-9 and SJ4-10 in the crack-free state is shown in Table 3.

Table 3
Principal stress amplitude at the weld toe of specimens

Specimen	Left (MPa)	Right (MPa)
SJ4-7	494.2	-
SJ4-8	363.7	388.7
SJ4-9	516	583.9
SJ4-10	273.5	338.8

One channel of the right strain gauge rosette in SJ4-7 was damaged after being pasted, so the principal stress at this point was not measured. It can be seen from Table 3 that the data measured under the same loading amplitude are different due to the influence of pasting process, the quality of glue and the flatness of base material after polishing, etc. However, the 7 sets of data are basically between 300MPa and 500MPa with the average of 422.7MPa.

The data measured in the test is the stress amplitude and the stress ratio is set to be - 1, while the model in the finite element is statically loaded. Therefore, it is necessary to take half of the average stress amplitude 211.4MPa to compare with that obtained by the finite element. The maximum principal stress extracted at nominal stress point A in the finite element model is 198.6 MPa. The error between the finite element and the test is only 6.1%, which shows good accuracy of using the finite element model for numerical simulation.

4.3. Maximum principal stress around hole

The maximum principal stress around the stop hole was extracted to draw the radar map. Placing the radar map at the hole can clearly reflect the distribution of the stress, as shown in Fig. 16(a). Plotting the stress extracted into a broken line according to the order of points can clearly reflect the relationship between the stress at the front and back side of the hole, as shown in Fig. 16(b). It can be seen from Fig. 16(a) and Fig. 16(b) that the high stress area at the crack tip is obviously larger than that in the front of the hole after drilling ahead of the crack. The principal stress in the front of the hole is larger than back side. The stress on the front side continues to increase as the fatigue crack grows. Stress concentration is even worse and the peak position of the maximum principal stress also changes.

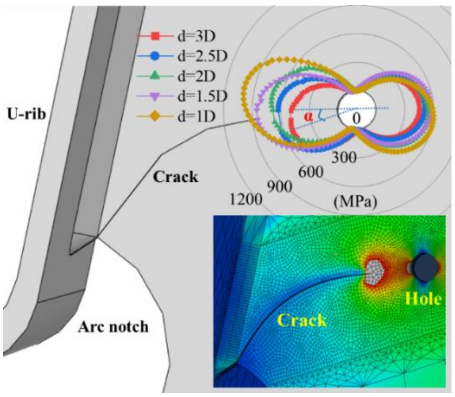

(a) Stress distribution around hole

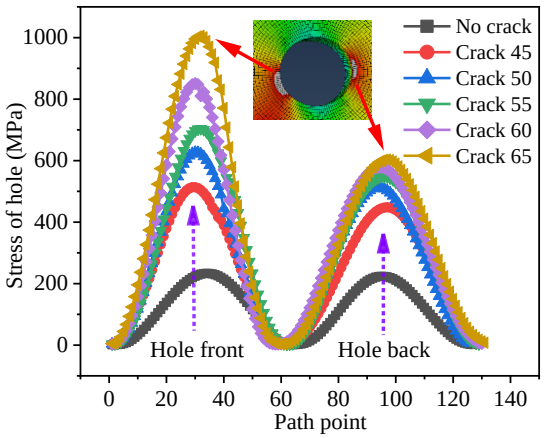

(b) Stress curve around hole

Fig. 16 Local stress after drilling ahead of the crack

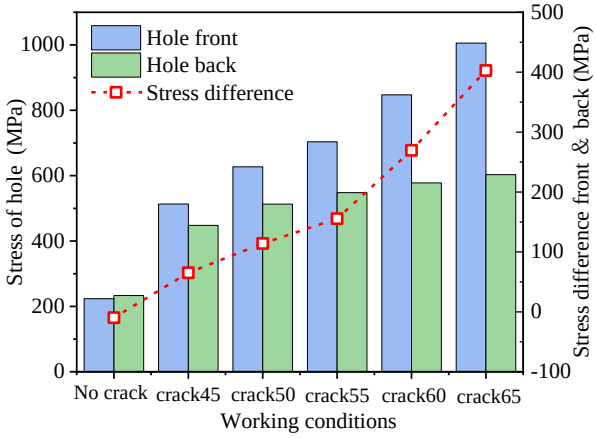

Fig. 17 Stress on the front and back side of the stop hole

The stress differences between the front and back of the hole under each working condition in Fig. 16(b) are calculated, as shown in Fig. 17. For drilling in the model without cracks, the maximum principal stress at the back of the stop hole is slightly greater than that at the front. Once cracks appear, the stress at the front of the hole turns to be greater than the back. With the fatigue crack propagation, the maximum principal stress at the back of the hole increases slowly and the growth rate is significantly lower than that at the front of the hole. The stress difference between two sides of the hole continues to increase. All the above simulations are highly consistent with that measured by strain gauges in the fatigue test in section 3.3.

The relationship between the strain difference of stop holes and crack length was established for SJ3-7, SJ3-8, SJ4-9 and SJ4-10 in section 3.3. The result extracted from fatigue tests and the finite element model was compared, as shown in Fig. 18. From the implementation of drilling to the cracking of stop hole, the strain difference on two sides of the hole continues to increase as the crack propagates. It is worth noting that there are obvious inflection points in curves. When the inflection point appears, the original crack has not reached the hole. At the inflection points of SJ3-7, SJ3-8, SJ4-9 and SJ4-10, the distance L (L = d - D/2) between the original crack tip and hole edge is 13mm, 11mm, 15mm and 10mm respectively. For the finite element model, L is 15mm, which is close to that in the test. This indicates that the high stress field at the crack tip will have a significant interference effect on the hole strain when the crack is within 15mm from the hole edge, which is the direct reason for the premature cracking of base metal at the front side of the hole.

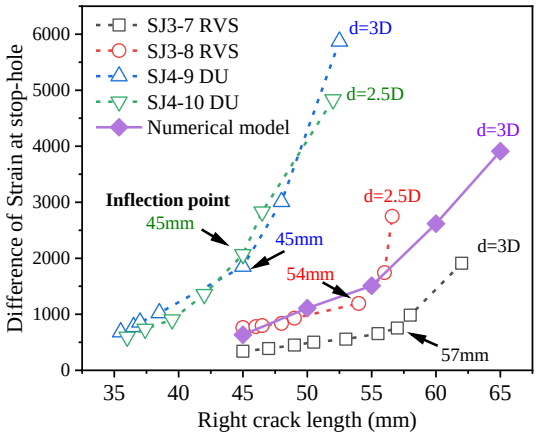

Fig. 18 Strain difference on the front and back side of the hole

4.4. Deflection of crack-growth path

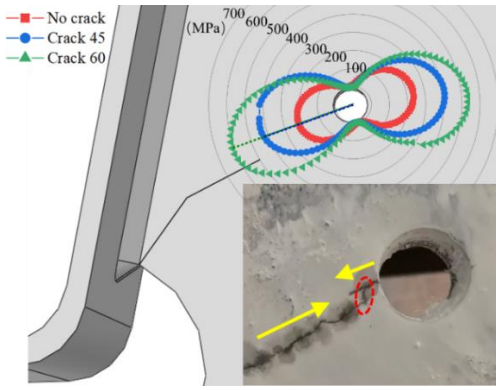

Fig. 19 Stress around the stop hole with an 5mm upward deviation

The relationship between the stress at hole edge and the crack length after moving the stop-hole 5mm above the fatigue crack-growth direction is shown in Fig. 19. If the stop-hole moves upward by 5mm, the extension line between the peak of principal stress and the hole center will be located above the fatigue crack, which is staggered from the crack-growth direction, as shown in Fig.19. Once the front side of the hole cracks, the crack will propagate along the extension line to the original crack, and crack turning will occur when two cracks intersect with each other, which illustrates the reason for the deflection of crack-growth path in real bridges and tests.

5. Conclusions

Based on fatigue test and finite element analysis, this paper analyzes the crack-propagation mode after drilling ahead of the crack tip. The conclusions are as follows:

1) After drilling ahead, crack propagation will damage the effective load-bearing section, resulting in continuous strain growth and significant stress

concentration at the hole. As the plastic zone at the crack tip covers hole edge, base material between the hole and crack yields. The hole will crack in advance, while original crack has not reached the hole. Then two cracks propagate towards each other at a rate twice that of the crack without drilling.

2) The high stress field at the crack tip has a significant interference effect on the strain at hole edge. In reverse, the stop hole can guide the crack to propagate towards the stress concentration zone in front of the hole, which is the reason for crack turning.

3) Compared with drilling at the crack tip, drilling ahead increases strain outside the hole to weaken the arresting effect and local stiffness. The stress intensity factors K_{I} and K_{II} at the crack tip are increased by 15%, which intensifies the crack propagation. However, crack retardation can still be observed after the original crack converges with the crack from hole.

4) For cracks propagating along the base material in real bridges, it is recommended to drill double holes at the crack tip and three times the hole diameter, so as to remove the tip as much as possible and avoid the poor arresting effect caused by misjudgment of the crack tip.

Acknowledgements

This research is supported by the National Key Research and Development Program of China (No. 2017YFE0128700).

References

[1] Guo T., Liu Z.X., Pan S.J. and Pan Z.H., "Cracking of longitudinal diaphragms in long-span cable-stayed bridges", Journal of Bridge Engineering, 20(11), 04015011, 2015. https://doi.org/10.1061/(ASCE)BE.1943-5592.0000771.

[2] Song Y.S., Ding Y.L., Wang G.X. and Li A.Q., "Fatigue-life evaluation of a high-speed railway bridge with an orthotropic steel deck integrating multiple factors", Journal of Performance of Constructed Facilities, 30(5), 04016036, 2016. https://doi.org/10.1061/(ASCE)CF.1943-5509.0000887.

[3] Berg N.V.D., Xin H. and Veljkovic M., "Effects of residual stresses on fatigue crack propagation of an orthotropic steel bridge deck", Materials & Design, 198, 109294, 2020. https://doi.org/10.1016/j.matdes.2020.109294.

[4] Wang Y.X., Fu Z.Q., Ge H.B., Ji B.H. and Norihiko H., "Cracking reasons and features of fatigue details in the diaphragm of curved steel box girder", Engineering Structures, 201, 109767, 2019. https://doi.org/10.1016/j.engstruct.2019.109767.

[5] Jie Z.Y., Wang W.J., Zhuge P., Li Y.D. and Wei X., "Fatigue properties of inclined cruciform welded joints with artificial pits", Advanced Steel Construction, 17(1), 20-27, 2021. https://doi.org/10.18057/IJASC.2021.17.1.3.

[6] Ayatollahi M.R., Razavi S.M.J. and Chamani H.R., "Fatigue life extension by crack repair using stop hole technique under pure mode-I and pure mode-II loading conditions", Procedia Engineering, 74, 18-21, 2014. https://doi.org/10.1016/j.proeng.2014.06.216.

[7] Reddy S., Vutkuru J., Madhavan M. and Kumar V., "Notch stress intensity factor for center cracked plates with crack stop hole strengthened using CFRP: A numerical study", Thin-Walled Structures, 98, 252-262, 2016. https://doi.org/10.1016/j.tws.2015.09.018.

[8] Ayatollahi M.R., Razavi S.M.J. and Yahya M.Y., "Mixed mode fatigue crack initiation and growth in a CT specimen repaired by stop hole technique", Engineering Fracture Mechanics, 145, 115-127, 2015. https://doi.org/10.1016/j.engfracmech.2015.03.027.

[9] Shin C.S., Wang C.M. and Song P.S., "Fatigue damage repair: a comparison of some possible methods", International Journal of fatigue, 18(8), 535-546, 1996. https://doi.org/10.1016/S0142-1123(96)00029-1.

[10] Yao Y., Ji B.H., Fu Z.Q., Zhou J. and Wang Y.X., "Optimization of stop hole parameters for cracks at diaphragm-to-rib weld in steel bridges", Journal of Constructional Steel Research, 162(5), 105747, 2019. https://doi.org/10.1016/j.jcsr.2019.105747.

[11] Fu Z.Q., Ji B.H., Xie S.H. and Liu T.J., "Crack stop holes in steel bridge decks: Drilling method and effects", Journal of Central South University, 24(10), 2372-2381, 2017. https://doi.org/10.1007/s11771-017-3649-8.

[12] Dexter R.J. and Ocel J.M., "Manual for repair and retrofit of fatigue cracks in steel bridges", McLean: The Federal Highway Administration, 2013. http://www.fhwa.dot.gov/bridge/steel/pubs/hif13020/hif13020.pdf.

[13] Wang Y.X., Ji B.H., Fu Z.Q. and Yao Y., "Fatigue repairing craftmanship of deck-to-vertical stiffener weld in the steel bridge deck", Advanced Steel Construction, 15(3), 232-241, 2019. https://doi.org/10.18057/IJASC.2019.15.3.3.

[14] Hu Y., Song M., Liu J. and Lei M., "Effects of stop hole on crack turning, residual fatigue life and crack tip stress field". Journal of the Brazilian Society of Mechanical Sciences and Engineering, 42(5), 1-14, 2020. https://doi.org/10.1007/s40430-020-02299-1.

[15] Makabe C., Murdani A., Kuniyoshi K., Irei Y. and Saimoto A., "Crack-growth arrest by redirecting crack growth by drilling stop holes and inserting pins into them", Engineering Failure Analysis, 16(1), 475-483, 2009. https://doi.org/10.1016/j.engfailanal.2008.06.009.

[16] Liu R., Liu Y.Q., Ji B.H. and Wang M.M., "Hot spot stress analysis on rib–deck welded joint in orthotropic steel decks", Journal of Constructional Steel Research, 97, 1-9, 2014. https://doi.org/10.1016/j.jcsr.2014.01.012.

[17] Xu Y.L., Shi Y.J., Wu Y.R. and Meng L.Y., "Residual stress of welded i sections fabricated from high performance steel: experimental investigation and modelling", Advanced Steel Construction, 15(1), 1-8, 2019. https://doi.org/10.18057/IJASC.2019.15.1.1.

[18] Jie Z.Y., Li Y.D., Wei X. and Zhuge P., "Fatigue life assessment of inclined welded joints in steel bridges subjected to combined normal and shear stresses", Advanced Steel Construction, 14(4), 620-633, 2018. https://doi.org/10.18057/IJASC.2018.14.4.6.

[19] Fisher J.W., Barthelemy B.M., Mertz D.R. and Edinger J.A., "Fatigue behavior of full-scale welded bridge attachments", Nchrp Report Transportation Research Board National Research Council Usa, 1980. http://onlinepubs.trb.org/Onlinepubs/nchrp/nchrp_rpt_227.pdf.

[20] Awad M.A., "Reducing plastic zone ahead of crack tips by reshaping stop hole", International Robotics & Automation Journal, 3(6), 00077, 2017. http://dx.doi.org/10.15406/iratj.2017.03.00077.

[21] Rooke D.P. and Cartwright D.J., Compendium of stress intensity factors, Her Majestyu2019s Stationery Office, London, 1976. https://doi.org/10.1017/S0001924000033923.

[22] Yuanzhou Z.Y., Ji B.H., Fu Z.Q., Kainuma S. and Tsukamoto S., "Fatigue crack retrofitting by closing crack surface", International Journal of Fatigue, 119, 229-237, 2019. https://doi.org/10.1016/j.ijfatigue.2018.10.006.

[23] KONDO. and Yoshiyuki., "Development of K-gage for stress intensity factor measurement", Transactions of the Japan Society of Mechanical Engineers, 53(495), 1977-1982, 1987. http://refhub.elsevier.com/S0142-1123(18)30634-0/h0110.

[24] Yamanishi M., Yamagami T., Tsukamoto S., Uesugi T., Fujita S. and Kannoto Y., "Proposal for prediction of fatigue crack propagation in steel bridges using K-gages", Bridge Management Systems, 2014. http://dx.doi.org/10.1201/b17063-23.

[25] Yao Y., Ji B.H., Li Y.F., Fu Z.Q. and Chen Z.Z., "Diaphragm splicing deviation in steel bridge deck: effect on fatigue performance and its preventive measures", Journal of Performance of Constructed Facilities, 35(3), 04021008, 2021. https://doi.org/10.1061/(ASCE)CF.1943-5509.0001572.

[26] Sciammarella C.A. and Sciammarella F.M., "Strain gage rosettes: selection, application and data reduction", John Wiley & Sons, Ltd, 2012. https://doi.org/10.1002/9781119994091.ch5.